

Electrical characterization of MgO tunnel barriers grown on InAs (001) epilayers

F. Magnus, S. K. Clowes, A. M. Gilbertson, W. R. Branford,
E. D. Barkhударov, and L. F. Cohen^{a)}

Blackett Laboratory, Imperial College, Prince Consort Road, London SW7 2AZ, United Kingdom

L. J. Singh, Z. H. Barber, and M. G. Blamire

Department of Materials Science and Metallurgy, University of Cambridge, Pembroke Street, Cambridge CB2 3QZ, United Kingdom

P. D. Buckle, L. Buckle, and T. Ashley

QinetiQ, Malvern Technology Centre, St. Andrews Road, Malvern WR14 3PS, United Kingdom

D. A. Eustace and D. W. McComb

Department of Materials, Imperial College, London SW7 2AZ, United Kingdom

(Received 27 June 2007; accepted 22 August 2007; published online 20 September 2007)

The authors examine the electrical properties of ultrathin MgO barriers grown on (001) InAs epilayers and the dependence on InAs surface pretreatment and growth conditions. Pretreatment improves the yield of tunnel junctions and changes the roughness of the interface between oxide and semiconductor. Electrical characterization confirms that tunnel barriers with appropriate values of interface resistance for efficient spin injection/detection have been achieved. Using the Rowell criteria and various tunneling models, the authors show that single step tunneling occurs above 150 K. Incorporating a thermal smearing model suggests that tunneling is the dominant transport process down to 10 K. © 2007 American Institute of Physics. [DOI: [10.1063/1.2784933](https://doi.org/10.1063/1.2784933)]

Control of spin in semiconductors remains highly topical.^{1–3} Although realizing the spin transistor⁴ or spin lifetime transistor⁵ has proved to be very difficult, certain concepts have now been shown to be robust and promising.³ Optimizing the results requires proper design of interfaces so that polarization is maintained efficiently across interfaces. Significant injection of spin from ferromagnetic (FM) metals into semiconductors (S) has been achieved for spin light-emitting diodes and it was with these devices that the need for a tunnel barrier injector^{6–8} was confirmed. Narrow gap semiconductors (NGSs) are attractive because of high electron mobility and strong spin-orbit coupling. Building compatible tunnel barriers between NGS and FM metals remains a challenge, particularly if one is to exploit the spin filtering properties of MgO in FM/oxide/S structures.⁹ MgO is also attractive because of its low barrier height.^{10,11} To harness the advantage offered by MgO, we must understand the electrical properties of MgO barriers grown on NGS which are as yet unexplored. Consequently, we have carried out a detailed study to determine the electrical integrity of structurally well characterized¹² MgO barriers with a specific aim to understand the influence of surface treatment and growth conditions. Importantly, we find that single step tunneling occurs through these barriers above 150 K rendering them effective for efficient injection or detection of spin. Moreover, taking thermal smearing into account indicates that tunneling is also the dominant transport process at low temperatures.

Thin MgO layers were deposited *ex situ* onto 1 μm thick epilayers of InAs(001)/GaAs grown by molecular beam epitaxy. One of three chemical surface treatments was carried out on the InAs prior to MgO deposition: (i) decrease in acetone and isopropanol, (ii) 18.5% HCl etch and 2.1%

(NH₄)₂S for surface passivation (single etch), (iii) recipe (ii) performed twice (double etch). The MgO was grown by reactive sputtering from a Mg target in an Ar–30% O₂ gas mixture. The substrate temperature during the MgO growth was 100 or 200 °C. After MgO growth, a 20 nm thick film of Co was deposited. Details of the growth and structural properties are given in Ref. 12.

The three Rowell criteria¹³ are commonly employed to show that tunneling is dominant: (i) The barrier current decays exponentially with increasing insulator thickness. (ii) The conductance spectrum $G(V)$ is nonlinear, as described by the Brinkman-Dynes-Rowell¹⁴ (BDR) model. (iii) The temperature dependence of the zero bias conductance $G_0(T)$ is weakly insulatorlike, as described by the Stratton model.¹⁵ However, recent studies have shown that criteria (i) and (ii) alone are not sufficient to rule out pinholes in a magnetic tunnel junction (MTJ).¹⁶ Furthermore, tunnel junctions can exhibit a sharp dip in conductance around zero bias.^{17,18} This is known as the zero bias anomaly (ZBA) and is usually attributed to resonant multistep tunneling via impurities which is not treated by the above models.

The BDR model is conveniently approximated at low bias voltages by a second order polynomial yielding three independent fitting parameters. These are generally taken to be the barrier thickness d , the mean barrier height ϕ , and the barrier asymmetry $\Delta\phi$. The BDR expression can be found in Ref. 14, Eq. (7). The Stratton model can give two independent parameters, generally d and ϕ , and is given in convenient form in Ref. 17, Eq. (5). Recently, however, Miller *et al.* have pointed out two severe shortcomings of Wentzel-Kramers-Brillouin-based tunneling models such as the BDR and Stratton models. Firstly, barrier roughness is not taken into account. Due to the first Rowell criterion, thinner regions will dominate resulting in lower d than expected and

^{a)}Electronic mail: l.cohen@imperial.ac.uk

TABLE I. Summary of sample properties. T_g is the growth temperature and t is the oxide thickness determined by TEM with ± 0.3 nm error.

Sample	Pretreatment	T_g (°C)	t (nm)	r_b ($\Omega \text{ m}^2$)	Tunneling
21472-1	Degreased	100	1.8	7.54×10^{-10}	no
21487-1	Degreased	200	1.8	1.13×10^{-10}	no
21527-1	Degreased	200	1.8	2.4×10^{-9}	yes
21358-2	Single etch	200	1.8	3.5×10^{-9}	yes
21424	Single etch	200	1.2	1.75×10^{-9}	yes
21472-2	Double etch	100	2.47×10^{-9}	yes	

greater φ .¹⁹ Secondly, the routinely employed expressions for the BDR and Stratton models use the free electron mass and do not take into account the effective electron mass m^* in the barrier material or conductor.²⁰ In a Co/MgO/InAs structure m^* varies by almost two orders of magnitude as $m^*/m_e=0.026$ in InAs.²¹

To obtain significant spin injection and detection, the interface resistance r_b needs at least to satisfy the condition $r_b \approx r_N = \rho_N l_{sf}$ where ρ_N is the resistivity and l_{sf} the spin diffusion length of the nonmagnetic material.^{2,6} The spin diffusion length in the nondegenerate limit can be defined as $(k_B T \mu \tau_{sf} / 2e)^{1/2}$ where μ is the mobility and τ_{sf} is the spin lifetime of the carriers. From a knowledge of the spin lifetime in bulk InAs,²² we can estimate the value of $r_b \approx 10^{-9} - 10^{-10} \Omega \text{ m}^2$ at room temperature. A direct interface between gold and InAs yields²³ an interface resistance of $\sim 10^{-12} \Omega \text{ m}^2$ and this leaves scope for growing a barrier material on the InAs to reach the desired r_b . From electrical characterization of MTJs, MgO tunnel barriers^{10,11} appear to have a relatively low barrier height of 0.9 eV. This allows us to predict, using the Simmons model,²⁴ that to achieve the desired r_b the target thickness of MgO should be ~ 1.3 nm on InAs. Table I shows a summary of the values for our samples with r_b varying from 3.5×10^{-9} to $1.1 \times 10^{-10} \Omega \text{ m}^2$ which is in the desired range for efficient spin injection and detection in a Co/MgO/InAs structure.

Conductance properties vary substantially but all surface preparation recipes produce junctions which show signs of tunneling. Figure 1 shows typical tunnelinglike $G(V)$ spectra from $T=10$ –300 K. $G(V)$ is parabolic at low V and high T , but below ~ 200 K a sharp dip in conductance appears to emerge around zero bias. This ZBA is present in almost all our tunneling spectra regardless of growth temperature and InAs pretreatment. The BDR model can therefore only be applied to the high T data and a fit to the 300 K curve is shown in the figure.

The right inset to Fig. 1 shows the temperature dependence of $G_0(T)$ for several junctions on the same wafer as shown in the main graph. There is an excellent agreement with the Stratton model above ~ 200 K and the temperature below which the ZBA emerges agrees with the full conductance curves. We find, in the high T regime, both a BDR-like $G(V)$ and a Stratton-like $G_0(T)$ which is a strong indication that tunneling is the dominant transport mechanism in these junctions at high T .

A recent study has shown that the temperature dependence of the ZBA can be explained by including the effects of thermal smearing on the tunneling process.²⁵ By taking the convolution of the low T data (10 K) with a Gaussian function,²⁶ we can simulate higher T curves and obtain the effective smearing temperature T^* required to reproduce

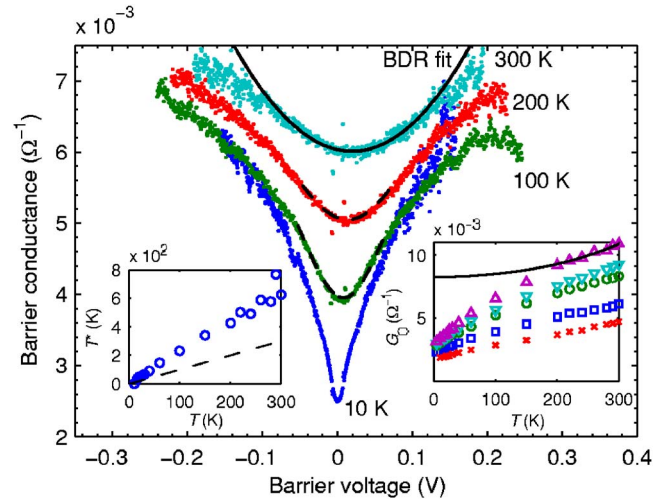


FIG. 1. (Color online) Typical barrier conductance spectra from room temperature down to 10 K showing parabolicity at high temperatures and the emergence of the ZBA at low temperatures. The solid line is a fit to the BDR model at 300 K. The right inset shows the temperature dependence of the zero bias conductance for several junctions on the same wafer. The solid line is a fit to the Stratton model above 200 K. The dashed lines in the main graph show the effect of thermally smearing the 10 K data allowing for a small offset in G and similarly a shift in V [for 100 K (200 K) $G_{\text{offset}} = 6 \times 10^{-4}$ (1.1×10^{-3}) Ω^{-1} and $V_{\text{offset}} = 6$ (12) mV]. The left inset shows the smearing temperature vs actual temperature.

higher T data, as shown by the dashed lines in Fig. 1. The left inset of Fig. 1 shows a T^* to T ratio of approximately 2 (the previous study finds a ratio of 1.6–2.0).

The absolute barrier parameters extracted from the fitting can only be treated as a guide to barrier properties due to the uncertainty in m^* . We fix the effective mass to $m^*/m_e = 0.1$ as this gives reasonable values for the fitting parameters. Thus, despite the uncertainty about their absolute values, we can use the fitting parameters as a guide to compare electrical variability between junctions of the same materials.

A spread in G_0 (at fixed T) between different junctions on each wafer is observed because of a variation in thickness (first Rowell criterion). Figure 2 shows the relationship between G_0 at 300 K and the thickness d , as determined by fitting to the BDR model. The relationship is indeed close to

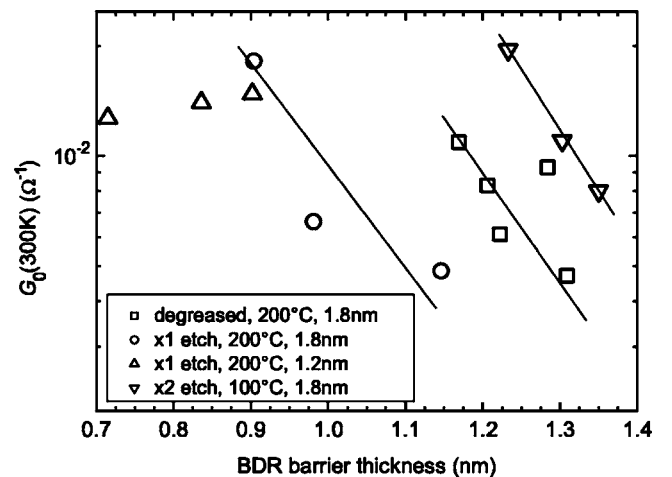


FIG. 2. Zero bias conductance at 300 K of each junction vs the barrier thickness as determined by fitting to the BDR model. The thicknesses in the legend are determined by TEM. The straight lines are a guide to the eye showing the expected exponential decay of G_0 .

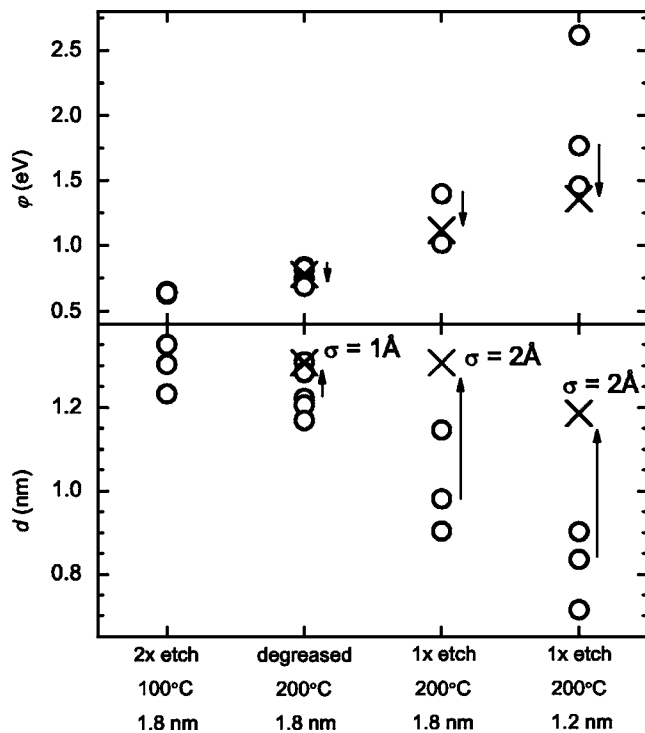


FIG. 3. Comparison of barrier thickness d and height ϕ determined by fitting to the BDR model for four different samples. The thickness determined by TEM is given below the x axis. The crosses show how barrier roughness σ can account for the apparent trend in d and ϕ .

exponential within each wafer except for the wafer with the thinnest barrier. Interestingly, we find a discontinuity in the $G_0(d)$ dependence between the wafers which we show can be attributed to the influence of barrier roughness. Perhaps not surprisingly, the mean thickness determined by TEM does not reflect the thickness relevant for electrical transport as indicated by the variation across the samples.

Figure 3 compares the barrier thickness d and height ϕ as determined by the BDR model for four different growth conditions and pretreatments. The trend of decreasing thickness and increasing barrier height seen across this series of samples corresponds to an increase in interface roughness as determined by TEM. The influence of roughness on the effective parameter values extracted using the BDR model has been discussed by Miller *et al.*¹⁹ We adopt this model and simulate roughness by assuming that the net conductance is the sum of parallel conductance channels with a Gaussian distribution of thicknesses with standard deviation σ . We take the sample series with the sharpest interface, the double etched sample, and use the mean extracted thickness of this series as a reference point. As shown in Fig. 3, we find that an increase in roughness of $\sigma=1$ Å (10%) and $\sigma=2$ Å (20%) can account for the apparent decrease in d and increase in ϕ for the degreased and single etched samples, respectively. The high roughness of the single etched samples is rein-

forced by conducting AFM which shows the presence of high current, pinholelike features.¹²

In summary, we have grown Co/ ~ 1.3 nm MgO/InAs trilayer structures with contact resistance values that are suitable for efficient spin injection/detection. The BDR and Stratton models have been used to determine whether tunneling dominates the conductance. A thermal smearing model gives further confirmation that tunneling dominates at all temperatures. Once the influence of roughness is taken into account, we find that the electrical properties of the barrier are relatively insensitive to surface pretreatment and growth temperature.

This work was supported by the UK-EPSC Grant No. EP/C511972 and EP/C511980. We thank Professor R. Magnus for valuable advice.

¹D. D. Awschalom and M. E. Flatte, Nat. Phys. **3**, 153 (2007).

²H. C. Koo, H. Yi, J. B. Ko, J. Chang, S. H. Han, D. Jung, S. G. Huh, and J. Eom, Appl. Phys. Lett. **90**, 022101 (2007).

³X. H. Lou, C. Adelman, S. A. Crooker, E. S. Garlid, J. Zhang, K. S. M. Reddy, S. D. Flexner, C. J. Palmstrom, and P. A. Crowell, Nat. Phys. **3**, 197 (2007).

⁴S. Datta and B. Das, Appl. Phys. Lett. **56**, 665 (1990).

⁵X. Cartoixa, D. Z. Y. Ting, and Y. C. Chang, Appl. Phys. Lett. **83**, 1462 (2003).

⁶A. Fert and H. Jaffres, Phys. Rev. B **6418**, 184420 (2001).

⁷E. I. Rashba, Phys. Rev. B **62**, R16267 (2000).

⁸G. Schmidt, D. Ferrand, L. W. Molenkamp, A. T. Filip, and B. J. van Wees, Phys. Rev. B **62**, R4790 (2000).

⁹X. Jiang, R. Wang, R. M. Shelby, R. M. Macfarlane, S. R. Bank, J. S. Harris, and S. S. P. Parkin, Phys. Rev. Lett. **94**, 056601 (2005).

¹⁰T. Kiyomura, Y. Maruo, and M. Gomi, J. Appl. Phys. **88**, 4768 (2000).

¹¹S. Mitani, T. Moriyama, and K. Takanashi, J. Appl. Phys. **93**, 8041 (2003).

¹²L. J. Singh, R. A. Oliver, Z. H. Barber, D. A. Eustace, D. W. McComb, S. K. Clowes, A. M. Gilbertson, F. Magnus, W. R. Branford, L. F. Cohen, L. Buckle, P. D. Buckle, and T. Ashley, J. Phys. D **40**, 3190 (2007).

¹³J. M. Rowell, in *Tunneling Phenomena in Solids*, edited by E. Burstein and S. Lundqvist (Plenum, New York, 1969), p. 273.

¹⁴W. F. Brinkman, R. C. Dynes, and J. M. Rowell, J. Appl. Phys. **41**, 1915 (1970).

¹⁵R. Stratton, J. Phys. Chem. Solids **23**, 1177 (1962).

¹⁶J. J. Akerman, J. M. Slaughter, R. W. Dave, and I. K. Schuller, Appl. Phys. Lett. **79**, 3104 (2001), and references therein.

¹⁷B. Oliver and J. Nowak, J. Appl. Phys. **95**, 546 (2004).

¹⁸L. Sheng, D. Y. Xing, and D. N. Sheng, Phys. Rev. B **70**, 094416 (2004).

¹⁹C. W. Miller, Z. P. Li, J. Akerman, and I. K. Schuller, Appl. Phys. Lett. **90**, 043513 (2007).

²⁰C. W. Miller, Z. P. Li, I. K. Schuller, R. W. Dave, J. M. Slaughter, and J. Akerman, Phys. Rev. B **74**, 212404 (2006).

²¹I. Vurgaftman, J. R. Meyer, and L. R. Ram-Mohan, J. Appl. Phys. **89**, 5815 (2001).

²²B. N. Murdin, K. Litvinenko, J. Allam, C. R. Pidgeon, M. Bird, K. Morrison, T. Zhang, S. K. Clowes, W. R. Branford, J. Harris, and L. F. Cohen, Phys. Rev. B **72**, 085346 (2005).

²³C. H. Moller, O. Kronenwerth, D. Grundler, W. Hansen, C. Heyn, and D. Heitmann, Appl. Phys. Lett. **80**, 3988 (2002).

²⁴J. G. Simmons, J. Appl. Phys. **34**, 1793 (1963).

²⁵J. J. Akerman, I. V. Roshchin, J. M. Slaughter, R. W. Dave, and I. K. Schuller, Europhys. Lett. **63**, 104 (2003).

²⁶Y. Bugoslavsky, Y. Miyoshi, S. K. Clowes, W. R. Branford, M. Lake, I. Brown, A. D. Caplin, and L. F. Cohen, Phys. Rev. B **71**, 104523 (2005).